iScience

CellPress
OPEN ACCESS

Article

Innate mechanism of mucosal barrier erosion in the pathogenesis of acquired colitis

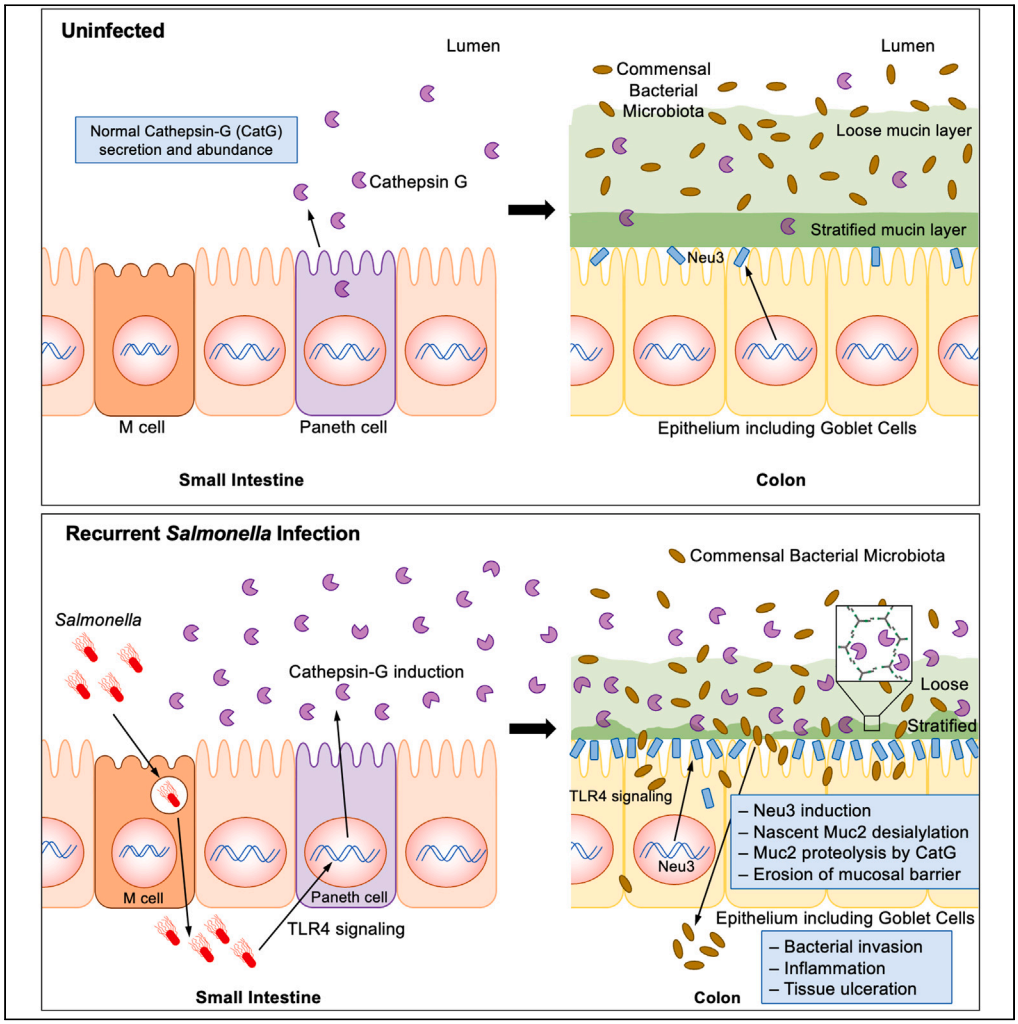

Won Ho Yang, Peter V. Aziz, Douglas M. Heithoff, ..., Michael J. Mahan, Markus Sperandio, Jamey D. Marth

bionicwono@yonsei.ac.kr (W.H.Y.)
jmarth@sbpdiscovery.org (J.D.M.)

Highlights

Recurrent Salmonella infection models acquired colitis and inflammatory bowel disease

Colonic mucosal barrier erosion with Mucin-2 proteolysis is a hallmark of colitis

Inductions of host Neu3 and Cathepsin-G are linked to increased Mucin-2 proteolysis

Loss of Neu3 or Cathepsin-G function protects against Mucin-2 proteolysis and colitis

Yang et al., iScience 26, 107883
October 20, 2023
https://doi.org/10.1016/j.isci.2023.107883

iScience

CellPress
OPEN ACCESS

Article

Innate mechanism of mucosal barrier erosion in the pathogenesis of acquired colitis

Won Ho Yang,[1,2,*] Peter V. Aziz,[1] Douglas M. Heithoff,[3] Yeolhoe Kim,[2] Jeong Yeon Ko,[2] Jin Won Cho,[2] Michael J. Mahan,[3] Markus Sperandio,[4] and Jamey D. Marth[1,5,*]

SUMMARY

The colonic mucosal barrier protects against infection, inflammation, and tissue ulceration. Composed primarily of Mucin-2, proteolytic erosion of this barrier is an invariant feature of colitis; however, the molecular mechanisms are not well understood. We have applied a recurrent food poisoning model of acquired inflammatory bowel disease using *Salmonella enterica* Typhimurium to investigate mucosal barrier erosion. Our findings reveal an innate Toll-like receptor 4-dependent mechanism activated by previous infection that induces Neu3 neuraminidase among colonic epithelial cells concurrent with increased Cathepsin-G protease secretion by Paneth cells. These anatomically separated host responses merge with the desialylation of nascent colonic Mucin-2 by Neu3 rendering the mucosal barrier susceptible to increased proteolytic breakdown by Cathepsin-G. Depletion of Cathepsin-G or Neu3 function using pharmacological inhibitors or genetic-null alleles protected against Mucin-2 proteolysis and barrier erosion and reduced the frequency and severity of colitis, revealing approaches to preserve and potentially restore the mucosal barrier.

INTRODUCTION

The maintenance and renewal of biophysical barriers within the body are essential for maintaining health. The mucosal barrier of the colon for example provides a physical separation between host cells and the microbes present in the intestinal lumen. This separation is essential to prevent host cell infection and tissue ulceration; consequently, the degradative breakdown of this barrier is a pathological hallmark of colitis and human inflammatory bowel disease (IBD).[1] Composed primarily of the sialylated Mucin-2 (Muc2) glycoprotein, the colonic mucosal barrier is produced by goblet cells that secrete processed mature Muc2 monomers as a disulfide-linked net-like polymer that expands with hydration at the lumenal surface of epithelial cells.[2] In the absence of Muc2, bacteria are observed in physical contact with epithelial cells and signs of inflammation and severe colitis develop early in life.[3,4] Nascent Muc2 polymers first contribute to the stratified (inner) mucin layer which forms the physical barrier between host epithelial cells and bacteria in the lumen.[5] As new Muc2 polymers are produced, previously secreted mucin layers are displaced outward from the epithelial cell surface and eventually undergo a progressive breakdown by glycolytic and proteolytic processes in the lumen becoming what is termed the loose (outer) mucin layer in which bacteria reside, forage, and thrive.[6] To maintain the mucosal barrier, the production and secretion kinetics of Muc2 polymers by goblet cells must closely match the rate of Muc2 polymer breakdown in the lumen.

As the major protein contributing to the colonic mucosal barrier, Muc2 is also a target of proteases that can be implicated in barrier erosion and the onset of colitis. Proteases of bacterial and protozoan origin have been reported capable of cleaving Muc2 in cell culture systems.[7,8] Additionally, proteases produced by the colonic microbiome or perhaps by host cells in response to infection and inflammation may participate in colonic mucosal barrier breakdown. We investigated among these possibilities using a recurrent food poisoning model of human IBD involving repeated low dose and non-lethal gastric infections of mice with *Salmonella enterica* Typhimurium (ST), a prevalent human foodborne pathogen.[9] Herein, we report the discovery of an innate host response induced by recurrent ST infection that elevates the rate of Muc2 proteolysis in the absence of a compensatory increase in Muc2 protein production. This pathogenic mechanism involves the sequential action of host neuraminidase and protease enzymes induced in disparate cell types. Inhibition of this mechanism blocks the elevation of Muc2 proteolysis, preserves the structure and function of the mucosal barrier, and reduces the frequency and severity of colitis.

[1]Sanford-Burnham-Prebys Medical Discovery Institute, Infectious and Inflammatory Diseases Center; La Jolla, CA 92037, USA
[2]Glycosylation Network Research Center and Department of Systems Biology, College of Life Science and Biotechnology, Yonsei University, 50 Yonsei-ro, Seodaemun-gu, Seoul 03722, Republic of Korea
[3]Department of Molecular, Cellular, and Developmental Biology, University of California, Santa Barbara, Santa Barbara, CA 93106, USA
[4]Walter Brendel Center for Experimental Medicine, Institute of Cardiovascular Physiology and Pathophysiology, Ludwig Maximilians University, Munich, Germany
[5]Lead contact
*Correspondence: bionicwono@yonsei.ac.kr (W.H.Y.), jmarth@sbpdiscovery.org (J.D.M.)
https://doi.org/10.1016/j.isci.2023.107883

RESULTS

Muc2 sialylation and desialylation in mucin layer proteolysis

Recurrent monthly low dose gastric ST infection of adult laboratory mice results in the development and progression of an enduring colitis (Figures S1A–S1E).[9] Prior to the 4th gastric ST infection, the stratified inner mucin layer was significantly eroded with reduced Muc2 protein levels coincident with bacterial invasion of the host epithelium and elevated permeability of the mucosal barrier (Figures 1A–1D and S1F). The induction of Muc2 RNA has been reported among goblet cells in response to various stimuli; however, goblet cell numbers were decreased as was previously observed, and *Muc2* RNA levels were not altered among colon tissue (Figure 1E).[9] Extracellular Muc2 was isolated by immunoprecipitation separately from stratified and loose mucin layers and analyzed using reducing and non-reducing gel electrophoresis to measure the abundance and integrity of Muc2. Induced proteolysis of Muc2 was found in the stratified and loose mucin layers following recurrent ST infection with the appearance of Muc2 fragments of approximately 100 and 200 kDa in reducing and non-reducing gel analyses, respectively (Figures 1F and 1G).

The Muc2 mucin domain is heavily sialylated during its synthesis and this posttranslational modification plays a role in modulating Muc2 proteolysis. Multiple sialyltransferases modify Muc2 during its biosynthesis and trafficking to the cell surface. For example, sialylation by the ST6GALNAC1 sialyltransferase produces α2-6 linkages of sialic acid that reduced Muc2 susceptibility to proteolytic degradation in the context of colonic microbial dysbiosis.[10] Other sialyltransferases produce α2-3 sialic acid linkages also found at high levels on Muc2. Glycoprotein sialylation levels can be compared using analytical lectins such as the *Sambucus nigra* agglutinin lectin that binds a subset of α2-6 sialic acid linkages, the *Maackia amurensis* lectin II that binds a subset of α2-3 sialic acid linkages, and the *Erythrina cristagalli* agglutinin, *Ricinus communis* agglutinin, and peanut agglutinin lectins that bind subsets of galactose linkages exposed upon the removal of sialic acids by neuraminidases.[9,11,12] Comparing lectin binding among mucin samples from healthy uninfected mice, Muc2 sialylation was significantly lower in the outer loose mucin layer compared to the inner stratified mucin layer, consistent with a progressive desialylation during Muc2 aging in the lumen. Recurrent ST infection further reduced the presence of sialic acid linkages on Muc2 as was also noted by elevated galactose exposure among Muc2 in both mucin layers (Figure 1H). Our results indicated that not all sialic acids were eliminated from Muc2 during this *in vivo* response; instead, these findings suggested an increase in the normal rate of lumenal Muc2 proteolysis in the context of previous ST infections.

We identified the mouse *St3gal6*-encoded ST3Gal6 sialyltransferase expressed among colon epithelial cells in the normal modification of nascent Muc2 with α2-3 sialic acid linkages. Reduced Muc2 sialylation in the absence of ST3Gal6 and among uninfected mice was linked to spontaneous Muc2 proteolysis and mucin barrier breakdown with the onset of colitis (Figure S2).[9] These findings reveal that the St3gal6 sialyltransferase adds α2-3 sialic acid linkages that protect Muc2 from premature proteolysis, while elevated Muc2 desialylation observed following ST infection among wild-type animals suggests the induction of one or more neuraminidases/sialidases. Because the ST pathogen used herein does not encode a neuraminidase enzyme, these findings infer the involvement of a neuraminidase originating from the commensal microbiota and/or the host.

Neu3 neuraminidase in Muc2 modification and proteolysis

Among mammalian neuraminidases, Neu3 protein levels were significantly induced at the colon epithelial cell surface in response to recurrent ST infection (Figure 2A). This induction quantitatively accounted for the majority of neuraminidase activity measured in colon tissue and was linked to the reduction of glycoprotein sialylation with exposure of underlying galactose at the colonic epithelial cell surface (Figures 2B and S3). In the absence of Neu3, Muc2 expression was not significantly altered, and erosion of the stratified layer was reduced, thereby maintaining stratified layer integrity and separation of bacteria to the loose mucin layer with improved barrier function (Figures 2C–2G). These findings were linked to the retention of Muc2 sialylation with reduced Muc2 proteolysis in both stratified and loose mucin layers (Figures 2H–2K). In comparing the protective effect of Neu3 deficiency to oral treatment with the neuraminidase inhibitor zanamivir (Figure S4), we found that both approaches similarly maintained Muc2 sialylation, reduced Muc2 proteolysis, and preserved stratified mucin layer integrity and function.

Desialylation renders Muc2 susceptible to an increased rate of proteolysis

Nascent Muc2 desialylation by Neu3 hydrolyzes a subset of Muc2 sialic acid linkages in elevating Muc2 susceptibility to proteolysis. We tested the proteolytic susceptibility of desialylated Muc2 among non-proteolyzed Muc2 immunoprecipitates isolated from the colonic stratified layer of wild-type uninfected mice. Isolated intact Muc2 was incubated with neuraminidase *ex vivo* either prior to or at the same time a protease source was added to the assay. The protease source was provided using Muc2-depleted intestinal lumenal extracts obtained from uninfected or previously infected cohorts. Muc2 proteolysis was detectable and measurable in this assay and was significantly increased among Muc2 preparations that had been previously desialylated (Figure 3A). A time course using this assay revealed that the rate of Muc2 proteolysis was doubled with desialylated Muc2 and was further elevated in the presence of lumenal extracts from previously infected animals (Figure 3B).

Serine protease activity with induction of Cathepsin-G in Muc2 proteolysis

To identify the protease(s) involved in increased Muc2 proteolysis, we similarly tested the effect of Muc2-depleted lumenal extracts in the presence of various protease inhibitors. We found that a combination of protease inhibitors was able to block Muc2 proteolysis; therefore, we separately applied selective inhibitors of different protease classes spanning cysteine proteases, serine proteases, and metalloproteases. Only the serine protease inhibitor blocked Muc2 proteolysis (Figure 4). The investigation of serine proteases within the intestinal tract

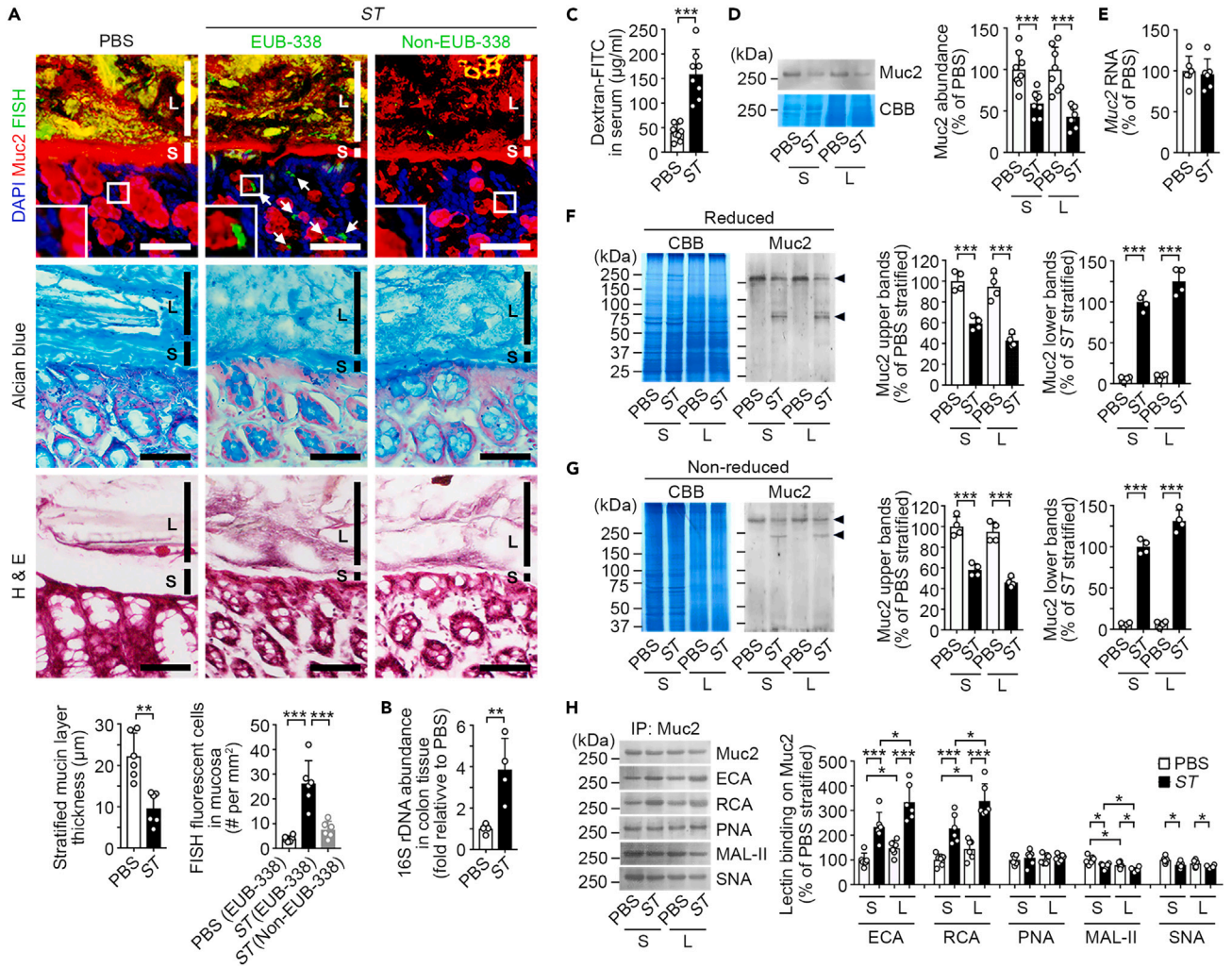

Figure 1. Recurrent *ST* infection is linked to colonic Muc2 desialylation, Muc2 proteolysis, and the erosion of the protective stratified mucin layer

Wild-type (WT) mice at 8 weeks of age were infected with *ST* (2×10^3 cfu) or uninfected (PBS) every 4 weeks for 6 consecutive months.

(A) Colon sections isolated from WT mice were incubated with antibodies to Muc2 (red), and then FISH staining for bacteria (green) was performed with EUB-338 probe that detected intact bacteria (white arrows) and a negative control probe (non-EUB-338). DNA is stained with DAPI (blue). In lower panels, colon sections were stained with Alcian blue and nuclear fast red, and separately, H&E. S, stratified inner mucin layer; L, loose outer mucin layer. Scale bars, 50 μm. The thickness of the stratified inner mucin layer and FISH fluorescent (EUB-338$^+$) cells in mucosa was quantified from 4 fields of view each from 6 wild-type mice including littermates with each condition.

(B) Relative abundance of bacterial 16S rDNA detected in colon tissues by real-time PCR using 16S universal primers (n = 4 mice with each condition).

(C) Intestinal epithelial barrier function (n = 8 mice with each condition).

(D) Immunoblot analysis of Muc2 protein in the colonic stratified (S) and loose (L) mucin layer (n = 8 mice with each condition).

(E) Muc2 mRNA expression in colon tissue (n = 6 mice with each condition).

(F and G) Immunoblot analysis of reduced and non-reduced Muc2 protein samples analyzed by corresponding polyacrylamide gel electrophoresis from the colonic stratified (S) and loose (L) mucin layers (n = 4 mice with each condition). Arrowheads to the right of the gels denote the positions of two major Muc2 protein bands detected by anti-Muc2 antibody.

(H) Lectin blot analysis from identical amount of Muc2 in the colonic stratified (S) and loose (L) mucin layer (n = 6 mice with each condition). Glycan linkages attached to Muc2 were analyzed using lectins including *Erythrina cristagalli* agglutinin (ECA) and *Ricinus communis* agglutinin (RCA-I/RCA) that both bind exposed galactose linkages, peanut agglutinin (PNA) that selectively binds the unsialylated Core 1 O-glycan, the *Maackia amurensis* lectin II (MAL-II) that detects a subset of α2-3 sialic acid linkages, and the *Sambucus nigra* agglutinin (SNA) that detects a subset of α2-6 sialic acid linkages.

(A–H) All mice were analyzed at 20 weeks of age prior to the fourth *ST* infection. Muc2 was visualized following denaturing (D, F, H) or non-denaturing (G) polyacrylamide gel electrophoresis. Plots are presented as means of biological replicates ±SD (*p < 0.05; **p < 0.01; ***p < 0.001).

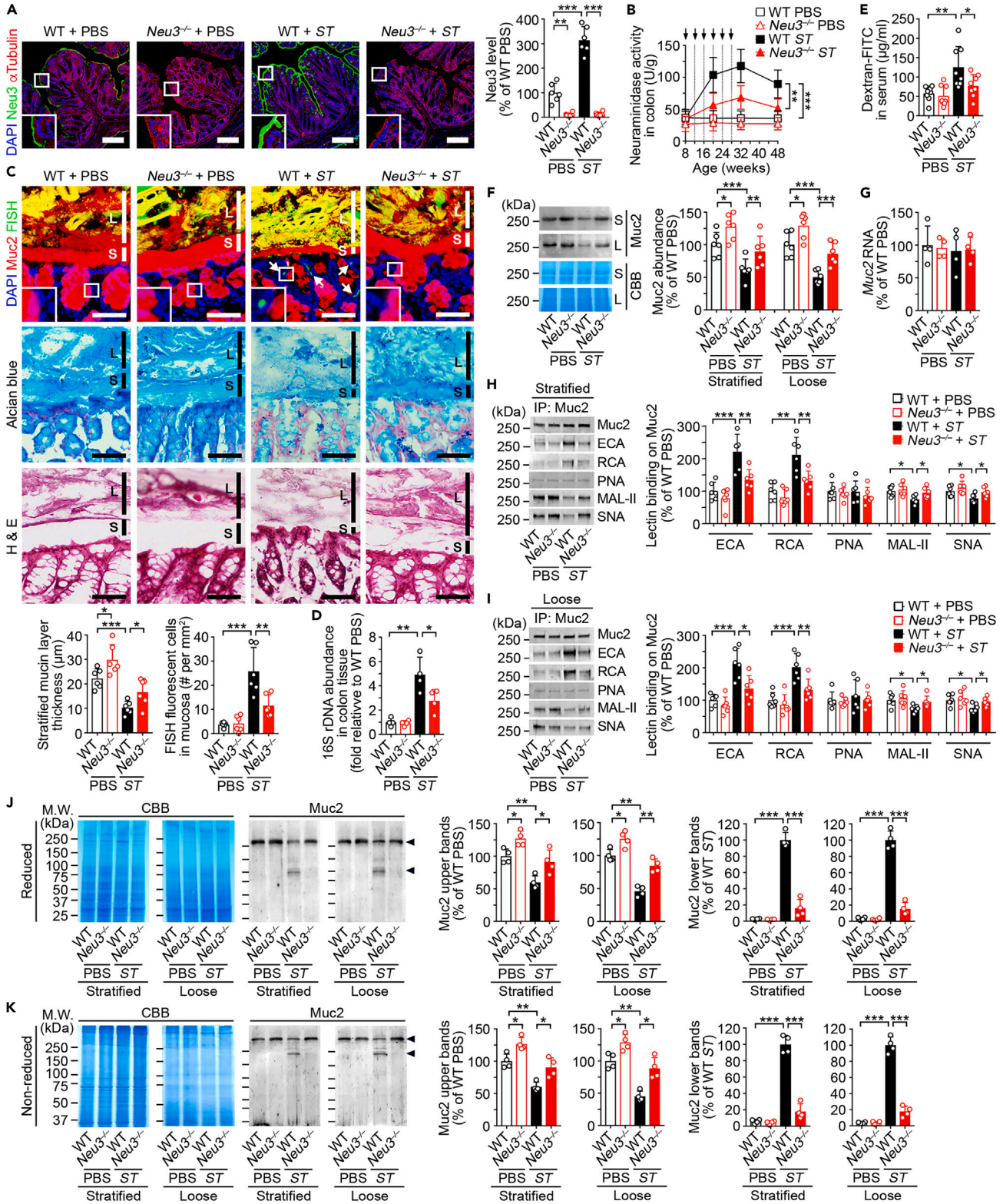
A
WT + PBS
Neu3−/− + PBS
WT + ST
Neu3−/− + ST
DAPI Neu3 αTubulin
Neu3 level (% of WT PBS)
B
WT PBS
Neu3−/− PBS
WT ST
Neu3−/− ST
Neuraminidase activity in colon (U/g)
Age (weeks)
E
Dextran-FITC in serum (μg/ml)
C
DAPI Muc2 FISH
Alcian blue
H & E
F
(kDa)
Muc2
CBB
Muc2 abundance (% of WT PBS)
Stratified
Loose
G
Muc2 RNA (% of WT PBS)
H
Stratified
IP: Muc2
ECA
RCA
PNA
MAL-II
SNA
Lectin binding on Muc2 (% of WT PBS)
I
Loose
Stratified mucin layer thickness (μm)
FISH fluorescent cells in mucosa (# per mm2)
D
16S rDNA abundance in colon tissue (fold relative to WT PBS)
J
M.W. (kDa)
CBB
Muc2
Reduced
Muc2 upper bands (% of WT PBS)
Muc2 lower bands (% of WT ST)
K
Non-reduced
PBS
ST

Figure 2. Colonic Neu3 neuraminidase induction in Muc2 desialylation and proteolysis

(A) *In situ* localization of Neu3 protein in colon sections of littermates of indicated genotypes and conditions. Neu3 protein is visualized using anti-Neu3 antibodies (green). Quantitation was analyzed from the average of 3–4 fields of view each from 6 independent mice each including littermates of each genotype and condition. Scale bars, 100 μm.

(B) Neuraminidase (Neu) activity measured from total tissue homogenates of the colon at multiple time points prior and subsequent to recurrent *ST* infection (n = 6 mice of each genotype and condition).

(C) Colon sections isolated from indicated genotypes were incubated with antibodies to Muc2 (red), and then FISH staining for bacteria (green) was performed with the EUB-338 probe. White arrows denote bacterial penetration in the colonic mucosa. Colon sections were also stained with Alcian blue and nuclear fast red, or H&E. S, stratified inner mucin layer; L, loose outer mucin layer. Scale bars, 50 μm. The thickness of the stratified inner mucin layer and FISH fluorescent (EUB-338^{+}) cells in mucosa were quantified from the average of 3–4 fields of view each from 6 independent mice including littermates of each genotype and condition.

(D) Relative abundance of bacterial 16S rDNA detected in colon tissues by real-time PCR using 16S universal primers (n = 4 mice per each genotype and condition).

(E) Intestinal epithelial barrier function (n = 8 mice per each genotype and condition).

(F) Immunoblot analysis of Muc2 protein in the colonic stratified (S) and loose (L) mucin layer (n = 6 mice per each genotype and condition).

(G) Muc2 mRNA expression in colon tissue (n = 4 mice per each genotype and condition).

(H and I) Lectin-binding analyses of glycan linkages from identical amounts of Muc2 in the colonic stratified and loose mucin (n = 6 mice per each genotype and condition).

(J and K) Immunoblot analyses of reduced and non-reduced Muc2 protein samples analyzed by corresponding polyacrylamide gel electrophoresis from the colonic stratified (S) and loose (L) mucin layers (n = 4 mice per each genotype and condition). Arrowheads to the right of the gels indicate two major Muc2 protein bands detected.

(A and C–K) Neu3-deficient mice and WT littermates at 20 weeks of age prior to the fourth *ST* infection. Muc2 was visualized following denaturing (F, H–J) or non-denaturing (K) polyacrylamide gel electrophoresis. Plots are presented as means of biological replicates ±SD (*$p < 0.05$; **$p < 0.01$; ***$p < 0.001$).

included three from host sources, namely Cathepsin-G (CatG), neutrophil elastase (NE), and proteinase 3 (PR3). NE and PR3 are produced mainly by neutrophils while CatG is also produced by Paneth cells of the small intestine.[13,14] From comparative studies of lumenal contexts of the total intestinal tract, we found that CatG was elevated 6-fold during recurrent ST infection, while NE and PR3 were elevated approximately 2-fold (Figure 5A). RNA transcripts encoding these proteases were similarly induced in small intestine tissue; however, CatG RNA was very low in the colon and was not elevated (Figure 5B). During the progression of disease in this colitis model, CatG protein levels in the lumen tracked upward with repeated ST infection and remained elevated following the cessation of recurrent infection (Figure 5C).

Histological analyses of the intestinal tract revealed CatG protein induction among epithelial cells within the crypts of the duodenum, jejunum, and ileum of the small intestine, with the noted absence of CatG protein in colon tissue (Figure 5D). The cell source of CatG was further identified using the Paneth cell marker lysozyme that colocalized with induced CatG (Figure 5E). Following secretion of CatG by Paneth cells, CatG was elevated in the lumenal contents of the small intestine and colon (Figure 5F). CatG protein induction was further detected in both the loose and stratified mucin layers of the colon, but not in tissue extracts of the colon (Figure 5G). The induction of CatG by Paneth cells was dependent upon Toll-like receptor 4 (Tlr4) function. Tlr4 deficiency abolished Neu3 induction on the colonic epithelium and protected against Muc2 proteolysis and erosion of the colonic mucosal barrier (Figure S5).

Cathepsin-G is required for induced Muc2 proteolysis and erosion of the mucosal barrier

The potential roles of CatG, NE, and PR3 in Muc2 proteolysis were investigated initially in our *ex vivo* assay using selective small-molecule inhibitors of these proteases. Only the CatG inhibitor significantly reduced Muc2 proteolysis (Figure 6A). A more definitive assignment of CatG as responsible for the induction of Muc2 proteolysis was sought by comparing mice lacking a functional CatG-encoding *Ctsg* gene. *Ctsg*-null mice appear normal without reported developmental abnormalities or spontaneous disease.[15] In our studies, the absence of CatG in *Ctsg*-null mice protected against colonic mucosal barrier erosion caused by recurrent ST infection with preservation of Muc2 expression and abundance (Figures 6B–6G). Muc2 proteolysis was significantly reduced in the absence of CatG in both stratified and loose mucin layers even though recurrent ST infection continued to desialylate Muc2 in the presence of elevated neuraminidase activity (Figures 6H, and S6A–S6C). The previously recorded 50% elevation of commensal microbial load in the intestinal tract following recurrent ST infection continued in CatG deficiency with increased abundance of gram-negative *Enterobacteriaceae* (Figure S6D).[9] The overgrowth of gram-negative *Enterobacteriaceae* following recurrent ST infection was also detected in CatG deficiency, indicating that this microbial dysbiosis was not responsible for significantly elevated Muc2 proteolysis or the severity of disease signs of acquired colitis in the presence of CatG further including fecal blood, diarrhea, and inflammatory cytokine expression (Figures 6H–6K).

DISCUSSION

The pathogenesis of colitis includes the proteolytic erosion of the protective colonic mucosal barrier. This process has been difficult to study and relatively little understanding exists of the mechanism(s) involved in barrier homeostasis. Using a repeated human food poisoning model of IBD originating from recurrent gastric ST infections, and with disease signs similar to human Ulcerative Colitis, we have identified an innate mechanism of colonic mucosal barrier erosion contributing to the onset and severity of acquired colitis. This sequential glycoproteolytic mechanism encompasses Tlr4-dependent induction of host Neu3 neuraminidase at the colonic epithelial cell surface resulting in the partial desialylation of nascent Muc2 glycoprotein produced by goblet cells. This desialylated Muc2 is more susceptible to proteolysis by lumenal

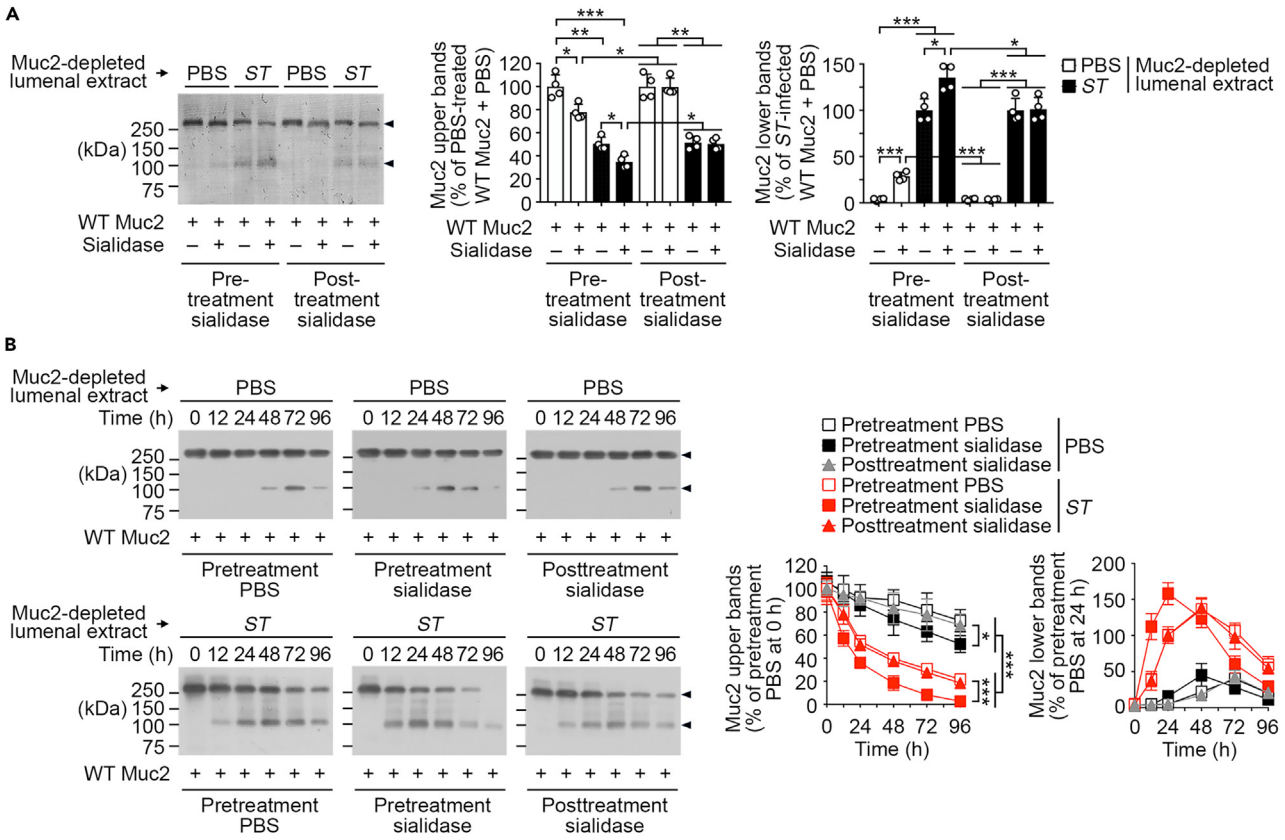

Figure 3. Prior Muc2 desialylation in altering the rate of Muc2 proteolysis

In vitro Muc2 proteolysis assay by pretreatment or posttreatment with *Arthrobacter urefaciens* sialidase (neuraminidase) (n = 4 mice of each condition).

(A and B) Muc2 immunoprecipitates isolated from the colonic stratified layer of WT mice at 12 weeks of age were treated with *Arthrobacter urefaciens* sialidase before or after incubation for 24 h (A) or indicated times (B) with Muc2-depleted lumenal extracts prepared from WT mice at 20 weeks of age prior to the fourth *ST* infection or PBS treatment. Muc2 was visualized following denaturing polyacrylamide gel electrophoresis. Arrowheads represent major Muc2 protein bands detected. Plots are presented as means of biological replicates ±SD (*p < 0.05; **p < 0.01; ***p < 0.001).

CatG. Neu3 absence or prolonged inhibition reduced Muc2 proteolysis preserving barrier maintenance with a pre-infection trend toward increased barrier thickness at steady state that may contribute to protection. Concurrently, host Tlr4 was required for the induction of CatG among Paneth cells of the small intestine, resulting in the secretion of CatG into the intestinal tract where it was found at elevated levels throughout the lumen including the colon. The basal rate of extracellular Muc2 proteolysis measured in healthy animals was significantly elevated in this model of acquired IBD. No compensatory increase in Muc2 protein level was detected likely because goblet cells were reduced in number and function as typical in chronic intestinal inflammation.[9,16] This contributes to a disequilibrium affecting Muc2 homeostasis consisting of an increased rate of Muc2 degradation in the absence of a compensatory increase in production, causing the progressive erosion of the colonic mucosal barrier.

Muc2 resistance to CatG proteolysis in the mouse colon is provided by the posttranslational modification of Muc2 by sialic acid linkages during its biosynthetic trafficking through the Golgi and prior to secretion by goblet cells. The critical dependence of mucosal barrier preservation on Muc2 sialylation by multiple sialyltransferases is indicated from our studies and from those reported among human IBD patients bearing an inherited deficiency of the ST6GalNAc1 sialyltransferase.[10] Similarly, inborn deficiency of the ST3Gal6 sialyltransferase, which produces only α2-3 sialic acid linkages, resulted in elevated Muc2 proteolysis, spontaneous barrier erosion, and colitis in the mouse.[9] The degree of Muc2 sialylation deficiency in one or more peptide sequence contexts may modulate the rate of Muc2 proteolysis and barrier breakdown. Compared with the absence of CatG, we found that oral treatment with the neuraminidase inhibitor zanamivir resulted in similar protection from elevated Muc2 proteolysis and barrier erosion. CatG was observed in the lumen of the colon at basal levels in wild-type mice, and may also operate as an antimicrobial factor. While CatG induction was the major source of the increased proteolysis of Muc2, the absence of CatG did not completely inhibit the induction of Muc2 proteolysis. Other host proteases including NE and PR3, or perhaps proteases originating from commensal microbes, may contribute more prominently in other contexts. The increased number of gram-negative *Enterobacteriaceae* observed has been linked to an acquired deficiency of host alkaline phosphatase.[9] In contrast with the present studies, CatG deficiency did not prevent the expansion of *Enterobacteriaceae* and was not as effective as alkaline phosphatase supplementation at blocking the induction

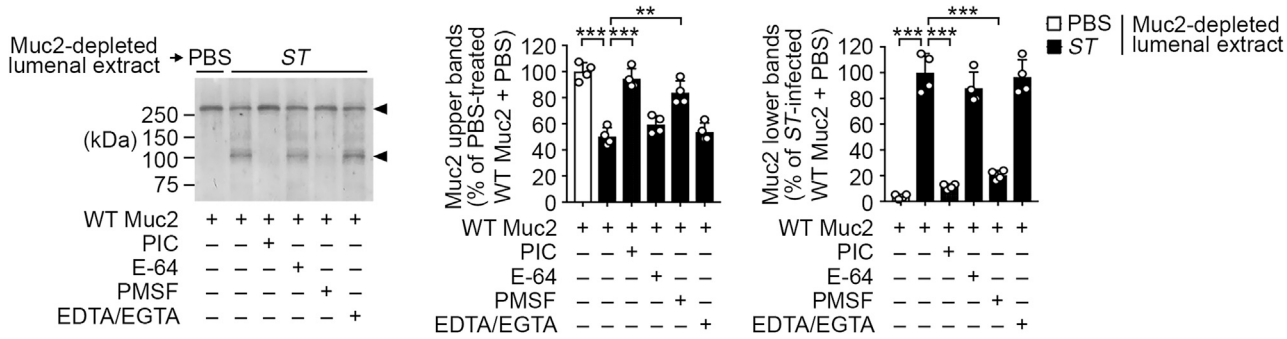

Figure 4. Selective inhibition of Muc2 proteolysis

Muc2 proteolysis was assayed in the absence or presence of various general protease inhibitors including a protease inhibitor cocktail (PIC), the cysteine protease inhibitor (E−64), the serine protease inhibitor (PMSF), and the metalloprotease inhibitor (EDTA/EGTA). Muc2 immunoprecipitates isolated from the colonic stratified layer of uninfected WT mice at 12 weeks of age were incubated with protease inhibitors in the presence of Muc2-depleted lumenal extracts prepared from either uninfected WT mice (PBS) or from infected littermates (ST) prior to the fourth *ST* infection or PBS treatment. Representative result is shown in left panel, while results from multiple animals is plotted on the right (n = 4 mice at 20 weeks of age with each condition). Muc2 was visualized following denaturing polyacrylamide gel electrophoresis. Plots are presented as means of biological replicates ±SD (**p < 0.01; ***p < 0.001).

of inflammatory cytokine expression. Therefore, the colonic microbial dysbiosis that involves *Enterobacteriaceae* does not contribute substantially to Muc2 proteolysis and barrier erosion in our repeated food poisoning model of acquired IBD.

Sialic acid linkages are posttranslational protein modifications bearing a negative charge in physiological conditions. The structure of Muc2 includes multiple domains including two "PTS" domains, often called mucin domains, rich in tripeptide repeats of proline, threonine, and serine. The two PTS/mucin domains of Muc2 harbor the greatest degree of glycosylation, predominantly O-glycosylation on multiple threonine and serine residues.[17,18] The O-glycans of nascent Muc2 are sialylated and the resulting high density of negative charge in the PTS domains is believed to contribute to the extended conformation of the Muc2 glycoprotein appearing as a "bottlebrush."[19] Deficiency in the formation of Core 1 and Core 3 O-glycans, which are mostly sialylated, resulted in a deficient and defective mucosal barrier with the development of colitis.[20,21] The partial elimination of sialic acid linkages and perhaps those normally residing on Core 1 and Core 3 O-glycans may occur at the cell surface where the majority of Neu3 induction is observed in proximity to nascent Muc2, and may occur during secretion. Deficient sialylation can occur from inherited genetic defects of sialyltransferases or the induction of neuraminidases, each decreasing Muc2 sialylation and an increased rate of proteolysis.

The colon is a tissue under constant threat from environmental toxins and infection. Muc2 is a key component of the stratified mucin layer protecting the colon from damage and disease. Recurrent ST infection induced Muc2 proteolysis resulting in mucosal barrier erosion in the onset of an acquired colitis that appears similar to human Ulcerative Colitis. The pathogenic mechanism includes innate Tlr4-dependent induction of colon epithelial cell Neu3 and Paneth cell CatG of the small intestine that act sequentially by removing Muc2 sialic acids that protect against increased Muc2 proteolysis and barrier degradation. Tlr4 has been shown essential also for the inflammation produced in this food poisoning model of IBD by causing the acquired depletion of the anti-inflammatory intestinal alkaline phosphatase (IAP).[9] CatG deficiency has a lesser effect on inflammatory cytokine induction than does IAP deficiency comparing with previous studies, which may reflect the efficacy of augmented IAP treatment in reducing LPS-P levels. Whether this mechanism operates in response to infection by other microbial species and in the context of other changes in the colonic microbiome remains to be known. In humans, this mechanism of disease may exist among some IBD patients with increased Neu3 neuraminidase and CatG serine protease levels reported.[22–24] This glycoproteolytic mechanism of colonic mucosal barrier erosion begins with the innate inflammatory response of the host to repeated gastric infection by the common foodborne ST bacterial pathogen and identifies potential therapeutic targets for inhibition to maintain and possibly restore the protective colonic mucosal barrier.

Limitations of this study

The structure of nascent secreted Muc-2 and its net-like polymeric organization in the stratified mucin layer under normal and pathogenic conditions remains under intense investigation. The murine Muc2 protein translated (accession number NP_076055.4) is composed of 4576 amino acids. Our findings using polyacrylamide gel electrophoresis demonstrate that colonic murine Muc2 isolated from the stratified mucin layer and visualized with commercially available antibody reagents migrates above the highest molecular weight marker used of 250 kDa in reducing polyacrylamide gel electrophoresis, and significantly larger in non-reducing conditions. Absent standard molecular weight markers are above 250 kDa; we do not know the precise molecular weight of Muc2 in these gel migration analyses. Other studies using polyacrylamide gel electrophoresis reported Muc2 migration at 200 kDa and above, or above 450 kDa.[25,26] Studies using agarose gel electrophoresis have reported Muc2 migration above the highest molecular weight markers used in each study, either 225, 250, or 460 kDa.[20,27,28] Another study reports Muc2 molecular weight above 540 kDa although the gel system used was not indicated.[29] There are multiple possible reasons for these differences that we cannot distinguish at present. First, agarose gel electrophoresis may more closely represent Muc2

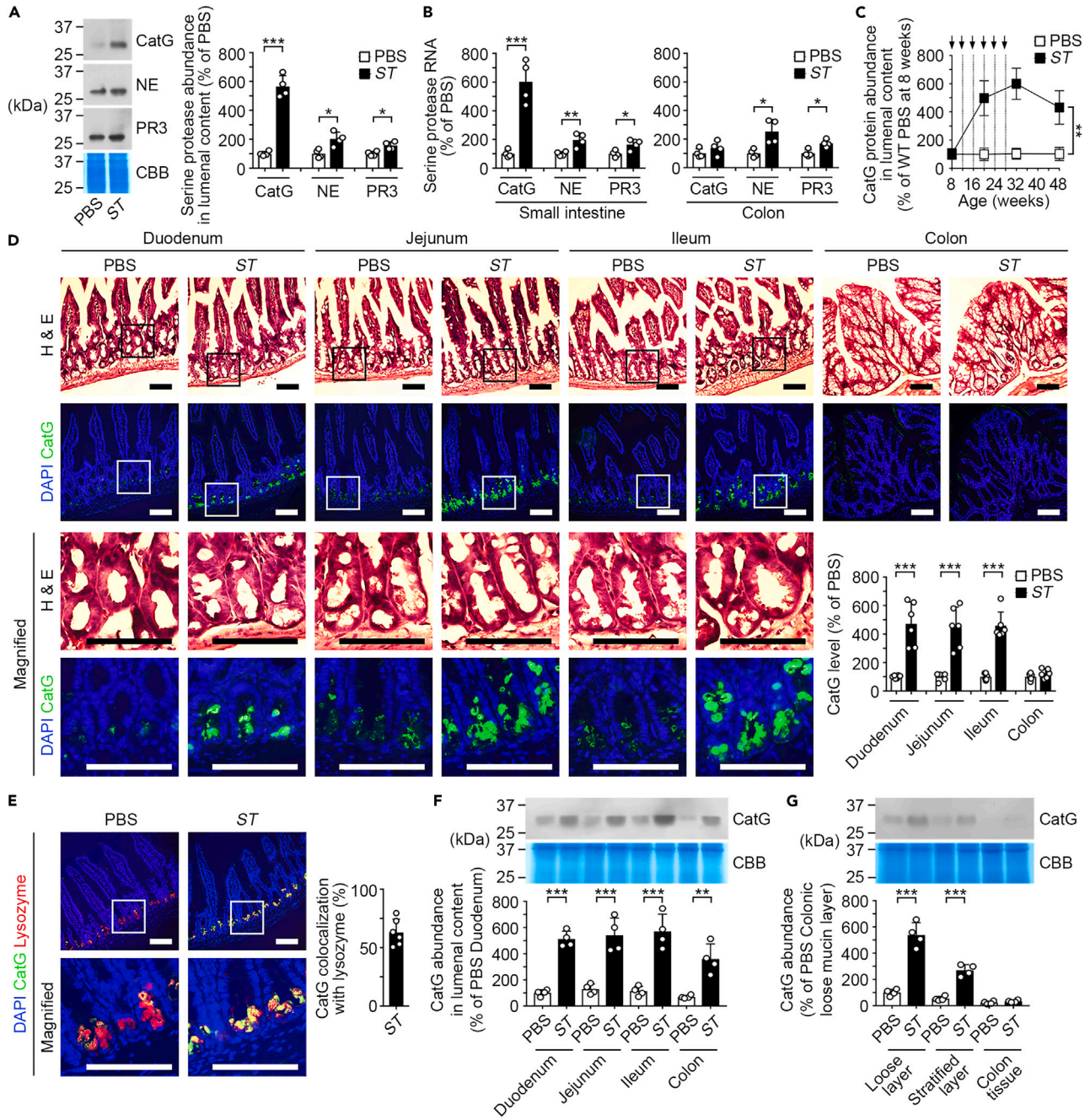

Figure 5. Serine protease expression is induced with Muc2 proteolysis

(A) Immunoblot analysis of different serine proteases including Cathepsin-G (CatG), neutrophil elastase (NE), and proteinase 3 (PR3) in the luminal content (n = 4 mice per each condition).

(B) mRNA expression of serine proteases in small intestine and colon tissue (n = 4 mice per each condition).

(C) Alterations in CatG protein abundance in the lumenal content of WT mice during *ST* reinfection (n = 4 mice per each condition).

(D) *In situ* localization of CatG protein in duodenum, jejunum, ileum, and colon sections stained with H&E or in fluorescent analyses with antibody to CatG (green) and DAPI staining of cell nuclei (blue). Quantitation was analyzed from the average of 3–4 fields of view each from 6 independent mice including littermates of each treatment condition. Scale bars, 100 μm.

(E) *In situ* localization of CatG and lysozyme in duodenum sections using antibodies to CatG (green) and lysozyme (red). Quantitation was analyzed from 3 to 4 fields of view each from 6 independent mice including littermates of each treatment condition. Scale bars, 100 μm.

(F) Immunoblot analyses of CatG protein levels present in intestinal contents isolated from indicated compartments of the intestine (n = 4 mice per each condition).

Figure 5. *Continued*

(G) Immunoblot analysis of CatG in the colonic stratified (S) and loose (L) mucin layers, and in colon tissue preparations following the removal of both mucin layers (n = 4 mice per each condition).

(A, B, D–G) WT mice at 20 weeks of age prior to the fourth *ST* infection.

(A, F, G) Proteins were visualized following denaturing polyacrylamide gel electrophoresis. Plots are presented as means of biological replicates ±SD (*$p < 0.05$; **$p < 0.01$; ***$p < 0.001$).

polymeric structure in the stratified layer, perhaps similar to our findings of Muc2 migration using non-reducing polyacrylamide electrophoresis. Second, secreted Muc2 may be normally processed into smaller forms by removal of terminal domain(s) during oligomerization and residence within in the stratified layer, rendering subsequent molecular weight analyses unrepresentative of primary amino acid sequence. Third, protein sialylation with the attendant negative charge can affect electrophoretic determinations of molecular weight. Finally, our findings as well as those of some others referenced may be detecting a processed fragment of the full-length translated Muc2 product that primarily contributes to the normal structure and functioning of the mucin barrier. Nevertheless, using pharmacological inhibition and genetic-null alleles, we have demonstrated that the induction of Muc2 proteolysis and erosion of the colonic mucosal barrier are linked to the functions of Neu3 and Cathepsin-G. Moreover, Neu3 and Cathepsin-G induction are further linked to an increased frequency of onset and severity of colitis using this repeated food poisoning model of acquired colitis and IBD.

STAR★METHODS

Detailed methods are provided in the online version of this paper and include the following:

- KEY RESOURCES TABLE
- RESOURCE AVAILABILITY
  - Lead contact
  - Materials availability
  - Data and code availability
- EXPERIMENTAL MODEL AND STUDY PARTICIPANT DETAILS
  - Laboratory animals
  - Bacterial strains and culture conditions
- METHOD DETAILS
  - Bacterial infections
  - Histology
  - mRNA preparation and quantification by real-time PCR
  - *In vivo* intestinal barrier function
  - Separation of loose and stratified mucus layer Muc2
  - Immunoprecipitation, immunoblotting, and lectin blotting
  - ELISA
  - Neuraminidase activity and inhibition
  - *In vitro* Muc2 proteolysis
  - Comparative studies of intestinal microbiota
- QUANTIFICATION AND STATISTICAL ANALYSIS

SUPPLEMENTAL INFORMATION

Supplemental information can be found online at https://doi.org/10.1016/j.isci.2023.107883.

ACKNOWLEDGMENTS

This research was funded by NIH grants AI151371, HL131474, and DK048247 (J.D.M.). Additional support was provided by the Yonsei Research Fund (2019-22-0020) and the National Research Foundation of Korea Ministry of Science, ICT and Future Planning NRF-2016R1A5A1010764 and NRF-2020R1A2C101232911 (W.H.Y. and J.W.C.).

AUTHOR CONTRIBUTIONS

J.D.M. and W.H.Y. designed the experimental strategies. J.D.M. supervised the project. W.H.Y., P.V.A., D.M.H., Y.K., and J.Y.K. performed the experiments and acquired data. All authors contributed to data analysis and manuscript preparation.

DECLARATION OF INTERESTS

The authors declare no conflicts of interest or financial interests.

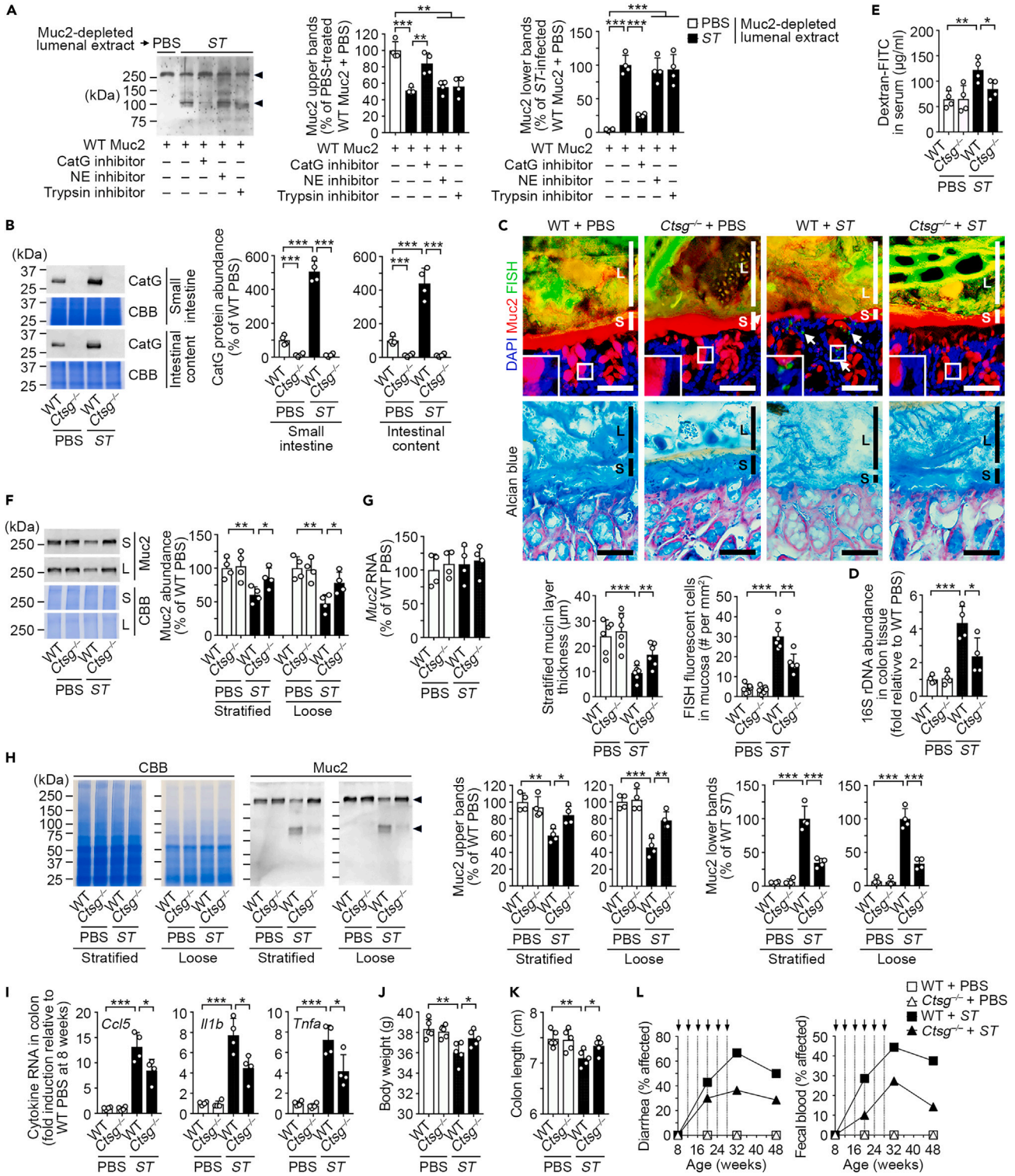

Figure 6. Pharmacological and genetic inhibition of Cathepsin-G

(A) Muc2 proteolysis using Muc2-depleted lumenal extracts in the absence or presence of selective protease inhibitors of CatG, NE, and Trypsin. Left panel provides a representative result (n = 4 mice per each condition). Arrowheads to the right of the gels denote positions of major Muc2 protein bands detected. (B) Immunoblot analysis of CatG protein levels in the small intestine tissue and in the lumenal intestinal contents of WT and CatG-deficient *Ctsg*-null littermates (n = 4 mice per each genotype and condition).

Figure 6. *Continued*

(C) Colon tissue sections were analyzed using antibody to Muc2 (red); FISH staining of bacteria (green) was performed with the EUB-338 probe. White arrows denote intact bacterial penetration into the colonic mucosa. Colon sections were also stained with Alcian blue and nuclear fast red. S, stratified inner mucin layer; L, loose outer mucin layer. Scale bars, 50 μm. The thickness of the stratified inner mucin layer and FISH fluorescent (EUB-338^{+}) cells in mucosa were averaged from 4 fields of view each from 6 independent mice including littermates of each genotype and condition.

(D) Relative abundance of bacterial 16S rDNA detected in colon tissues by real-time PCR using 16S universal primers (n = 4 mice per each genotype and condition).

(E) Intestinal barrier function (n = 4 mice per each genotype and condition).

(F) Immunoblot analysis of Muc2 protein in the colonic stratified (S) and loose (L) mucin layer (n = 4 mice per each genotype and condition).

(G) Muc2 mRNA expression in colon tissue (n = 4 mice per each genotype and condition).

(H) Immunoblot analyses of Muc2 proteolysis in the colonic stratified (S) and loose (L) mucin layer (n = 4 mice per each genotype and condition).

(I) Inflammatory cytokine mRNA expression in isolated colon tissue (n = 4 mice per each genotype and condition).

(J and K) Body weight and colon length (n = 5 male mice per each genotype and condition).

(L) Frequency of diarrhea (n = 12) and frequency of fecal blood detected (n = 12) were plotted throughout 48 weeks of age of adult life in the course of recurrent *ST* infections (arrows).

(B–I) *Ctsg*-null mice and WT littermates at 20 weeks of age prior to the fourth *ST* infection.

(J and K) *Ctsg*-null mice and WT littermates at 48 weeks of age.

(A, B, F, H) Proteins were visualized following denaturing polyacrylamide gel electrophoresis. Plots are presented as means of biological replicates ±SD (*$p < 0.05$; **$p < 0.01$; ***$p < 0.001$).

INCLUSION AND DIVERSITY

We support inclusive, diverse, and equitable conduct of research.

Received: January 26, 2023
Revised: August 16, 2023
Accepted: September 7, 2023
Published: September 9, 2023

REFERENCES

1. Bankole, E., Read, E., Curtis, M.A., Neves, J.F., and Garnett, J.A. (2021). The relationship between mucins and Ulcerative Colitis: A systemic review. J. Clin. Med. *10*, 1935. https://doi.org/10.3390/jcm10091935.
2. Hansson, G.C., and Johansson, M.E. (2010). The inner of the two Muc2 mucin-dependent layers in colon is devoid of bacteria. Gut Microb. *1*, 51–54. https://doi.org/10.4161/gmic.1.1.10470.
3. Van der Sluis, M., De Koning, B.A.E., De Bruijn, A.C.J.M., Velcich, A., Meijerink, J.P.P., Van Goudoever, J.B., Büller, H.A., Dekker, J., Van Seuningen, I., Renes, I.B., and Einerhand, A.W.C. (2006). Muc2-deficient mice spontaneously develop colitis, indicating that Muc2 is critical for colonic protection. Gastroenterology *131*, 117–129. https://doi.org/10.1053/j.gastro.2006.04.020.
4. Wenzel, U.A., Magnusson, M.K., Rydström, A., Jonstrand, C., Hengst, J., Johansson, M.E.V., Velcich, A., Öhman, L., Strid, H., Sjövall, H., et al. (2014). Spontaneous colitis in Muc2-deficient mice reflects clinical and cellular features of active Ulcerative Colitis. PLoS One *9*, e100217. https://doi.org/10.1371/journal.pone.0100217.
5. Johansson, M.E.V., Phillipson, M., Petersson, J., Velcich, A., Holm, L., and Hansson, G.C. (2008). The inner of the two Muc2 mucin-dependent mucus layers in colon is devoid of bacteria. Proc. Natl. Acad. Sci. USA *105*, 15064–15069. https://doi.org/10.1073/pnas.0803124105.
6. Johansson, M.E.V., Larsson, J.M.H., and Hansson, G.C. (2011). The two mucus layers of solon are organized by the MUC2 mucin, wheras the outer layer is a legislator of host-microbial interactions. Proc. Natl. Acad. Sci. USA *108*, 4659–4665. https://doi.org/10.1073/pnas.1006451107.
7. Lidell, M.E., Moncada, D.M., Chadee, K., and Hansson, G.C. (2006). Entamoeba histolytica cysteine proteases cleave the MUC2 mucin in its C-terminal domain and dissolve the protective colonic mucus gel. Proc. Natl. Acad. Sci. USA *103*, 9298–9303. https://doi.org/10.1073/pnas.0600623103.
8. Van der Post, S., Subramani, D.B., Bäckström, M., Johansson, M.E.V., Vester-Christensen, M.B., Mandel, U., Bennett, E.P., Clausen, H., Dahlén, G., Sroka, A., et al. (2013). Site-specific O-glycosylation on the MUC2 mucin protein inhibits cleavage by the Porphyromonas gingivalis secreted cysteine protease (RgpB). J. Biol. Chem. *288*, 14636–14646. https://doi.org/10.1074/jbc.M113.459479.
9. Yang, W.H., Heithoff, D.M., Aziz, P.V., Sperandio, M., Nizet, V., Mahan, M.J., and Marth, J.D. (2017). Recurrent infection progressively disables host protection against intestinal inflammation. Science *358*, eaao5610. https://doi.org/10.1126/science.aao5610.
10. Yao, Y., Kim, G., Shafer, S., Chen, Z., Kubo, S., Ji, Y., Luo, J., Yang, W., Perner, S.P., Kanellopoulou, C., et al. (2022). Mucus sialylation determines intestinal host-commensal homeostasis. Cell *185*, 1172–1188.e28. https://doi.org/10.1016/j.cell.2022.02.013.
11. Grewal, P.K., Uchiyama, S., Ditto, D., Varki, N., Le, D.T., Nizet, V., and Marth, J.D. (2008). The Ashwell receptor mitigates the lethal coagulopathy of sepsis. Nat. Med. *14*, 648–655. https://doi.org/10.1038/nm1760.
12. Yang, W.H., Aziz, P.V., Heithoff, D.M., Mahan, M.J., Smith, J.W., and Marth, J.D. (2015). An intrinsic mechanism of secreted protein aging and turnover. Proc. Natl. Acad. Sci. USA *112*, 13657–13662. https://doi.org/10.1073/pnas.1515464112.
13. Korkmaz, B., Horwitz, M.S., Jenne, D.E., and Gauthier, F. (2010). Neutrophil Elastase, Proteinase 3, and Cathepsin-G as therapeutic targets in human diseases. Pharmacol. Rev. *62*, 726–759. https://doi.org/10.1124/pr.110.002733.
14. Zamolodchikova, T.S., Tolpygo, S.M., and Svirshchevskaya, E.V. (2020). Cathepsin G-Not only inflammation: The immune protease can regulate normal physiological processes. Front. Immunol. *11*, 411. https://doi.org/10.3389/fimmu.2020.00411.
15. MacIvor, D.M., Shapiro, S.D., Pham, C.T., Belaaouaj, A., Abraham, S.N., and Ley, T.J. (1999). Normal neutrophil function in Cathepsin G-deficient mice. Blood *94*, 4282–4293.
16. Singh, V., Johnson, K., Yin, J., Lee, S., Lin, R., Yu, H., Rong, Y., In, J., Foulke-Abel, J., Zachos, N.C., and Donowitz, M. (2022). Chronic inflammation in Ulcerative Colitis causes long-term changes in Goblet cell function. Cell. Mol. Gastroenterol. Hepatol. *13*, 219–232. https://doi.org/10.1016/j.jcmgh.2021.08.010.
17. Arike, L., Holmén-Larsson, J., and Hansson, G.C. (2017). Intestinal Muc2 mucin O-glycosylation is affected by microbiota and regulated by differential expression of glycosyltransferases. Glycobiology *27*, 318–328. https://doi.org/10.1093/glycob/cww134.

18. Bergstrom, K.S.B., and Xia, L. (2013). Mucin-type O-glycans and their roles in intestinal homeostasis. Glycobiology *23*, 1026–1037. https://doi.org/10.1093/glycob/cwt045.
19. Arike, L., and Hansson, G.C. (2016). The densely O-glycosylated MUC2 mucin protects the intestine and provides food for the commensal bacteria. J. Mol. Biol. *428*, 3221–3229. https://doi.org/10.1016/j.jmb.2016.02.010.
20. Bergstrom, K., Fu, J., Johansson, M.E.V., Liu, X., Gao, N., Wu, Q., Song, J., McDaniel, J.M., McGee, S., Chen, W., et al. (2017). Core 1- and core 3-derived O-glycans collectively maintain the colonic mucus barrier and protect against spontaneous colitis in mice. Mucosal Immunol. *10*, 91–103. https://doi.org/10.1038/mi.2016.45.
21. Fu, J., Wei, B., Wen, T., Johansson, M.E.V., Liu, X., Bradford, E., Thomsson, K.A., McGee, S., Mansour, L., Tong, M., et al. (2011). Loss of intestinal core 1-derived O-glycans causes spontaneous colitis in mice. J. Clin. Invest. *121*, 1657–1666. https://doi.org/10.1172/JCI45538.
22. Denadai-Souza, A., Bonnart, C., Tapias, N.S., Marcellin, M., Gilmore, B., Alric, L., Bonnet, D., Burlet-Schiltz, O., Hollenberg, M.D., Vergnolle, N., and Deraison, C. (2018). Functional proteomic profiling of secreted serine proteases in health and inflammatory Bowel Disease. Sci. Rep. *8*, 7834. https://doi.org/10.1038/s41598-018-26282-y.
23. Jablaoui, A., Kriaa, A., Mkaouar, H., Akermi, N., Soussou, S., Wysocka, M., Wołoszyn, D., Amouri, A., Gargouri, A., Maguin, E., et al. (2020). Fecal Serine Protease Profiling in Inflammatory Bowel Diseases. Front. Cell. Infect. Microbiol. *10*, 21. https://doi.org/10.3389/fcimb.2020.00021.
24. Miklavcic, J.J., Hart, T.D.L., Lees, G.M., Shoemaker, G.K., Schnabl, K.L., Larsen, B.M.K., Bathe, O.F., Thomson, A.B.R., Mazurak, V.C., and Clandinin, M.T. (2015). Increased catabolism and decreased unsaturation of ganglioside in patients with Inflammatory Bowel Disease. World J. Gastroenterol. *21*, 10080–10090. https://doi.org/10.3748/wjg.v21.i35.10080.
25. Nishida, K., Kamizato, M., Kawai, T., Masuda, K., takeo, K., Teshima-Kondo, S., Tanahashi, T., and Rokutan, K. (2009). Interleukin-18 is a crucial determinant of vulnerability of the mouse rectum to psychosocial stress. Faseb. J. *23*, 1797–1805. https://doi.org/10.1096/fj.08-125005.
26. Wu, H., Chen, Q.Y., Wang, W.Z., Chu, S., Liu, X.X., Liu, Y.J., Tan, C., Zhu, F., Deng, S.J., Dong, Y.L., et al. (2021). Compound sophorae decoction enhances intestinal barrier function of dextran sodium sulfate induced colitis via regulating notch signaling pathway in mice. Biomed. Pharmacother. *133*, 110937. https://doi.org/10.1016/j.biopha.2020.110937.
27. Nyström, E.E.L., Arike, L., Ehrencrona, E., Hansson, G.C., and Johansson, M.E.V. (2019). Calcium-activated chloride channel regulator 1 (CLCA1) forms non-covalent oligomers in colonic mucus and has mucin-2 processing properties. J. Biol. Chem. *294*, 17075–17089. https://doi.org/10.1074/jbc.RA119.009940.
28. Sharpen, J.D.A., Dolan, B., Nyström, E.E.L., Birchenough, G.M.H., Arike, L., Martinez-Abad, B., Johansson, M.E.V., Hansson, G.C., and Recktenwald, C.V. (2022). Transglutaminase 3 crosslinks the secreted gel-forming mucus component Mucin-2 and stabilizes the colonic mucus layer. Nat. Commun. *13*, 45. https://doi.org/10.1038/s41467-021-27743-1.
29. Liu, Y., Lv, J., Liu, J., Li, M., Xie, J., Lv, Q., Deng, W., Zhou, N., Zhou, Y., Song, J., et al. (2020). Mucus production stimulated by IFN-AhR signaling triggers hypoxia of COVID-19. Cell Res. *30*, 1078–1087. https://doi.org/10.1038/s41422-020-00435-z.
30. Yamaguchi, K., Shiozaki, K., Moriya, S., Koseki, K., Wada, T., Tateno, H., Sato, I., Asano, M., Iwakura, Y., and Miyagi, T. (2012). Reduced susceptibility to colitis-associated colon carcinogenesis in mice lacking plasma membrane-associated sialidase. PLoS One *7*, e41132. https://doi.org/10.1371/journal.pone.0041132.
31. Yang, W.H., Nussbaum, C., Grewal, P.K., Marth, J.D., and Sperandio, M. (2012). Coordinated roles of ST3Gal-VI and ST3Gal-IV sialyltransferases in the synthesis of selectin ligands. Blood *120*, 1015–1026. https://doi.org/10.1182/blood-2012-04-424366.
32. Heithoff, D.M., Shimp, W.R., House, J.K., Xie, Y., Weimer, B.C., Sinsheimer, R.L., and Mahan, M.J. (2012). Intraspecies variation in the emergence of hyperinfectious bacterial strains in nature. PLoS Pathog. *8*, e1002647. https://doi.org/10.1371/journal.ppat.1002647.
33. Gerlach, K., Hwang, Y., Nikolaev, A., Atreya, R., Dornhoff, H., Steiner, S., Lehr, H.A., Wirtz, S., Vieth, M., Waisman, A., et al. (2014). TH9 cells that express the transcription factor PU.1 drive T cell-mediated colitis via IL-9 receptor signaling in intestinal epithelial cells. Nat. Immunol. *15*, 676–686. https://doi.org/10.1038/ni.2920.
34. Stone, E.L., Ismail, M.N., Lee, S.H., Luu, Y., Ramirez, K., Haslam, S.M., Ho, S.B., Dell, A., Fukuda, M., and Marth, J.D. (2009). Glycosyltransferase function in core 2-type protein O glycosylation. Mol. Cell Biol. *29*, 3770–3782. https://doi.org/10.1128/MCB.00204-09.
35. Ellies, L.G., Ditto, D., Levy, G.G., Wahrenbrock, M., Ginsburg, D., Varki, A., Le, D.T., and Marth, J.D. (2002). Sialyltransferase ST3Gal-IV operates as a dominant modifier of hemostasis by concealing asialoglycoprotein receptor ligands. Proc. Natl. Acad. Sci. USA *99*, 10042–10047. https://doi.org/10.1073/pnas.142005099.
36. Fuhrer, A., Sprenger, N., Kurakevich, E., Borsig, L., Chassard, C., and Hennet, T. (2010). Milk sialyllactose influences colitis in mice through selective intestinal bacterial colonization. J. Exp. Med. *207*, 2843–2854. https://doi.org/10.1084/jem.20101098.
37. Man, S.M., Zhu, Q., Zhu, L., Liu, Z., Karki, R., Malik, A., Sharma, D., Li, L., Malireddi, R.K.S., Gurung, P., et al. (2015). Critical Role for the DNA Sensor AIM2 in Stem Cell Proliferation and Cancer. Cell *162*, 45–58. https://doi.org/10.1016/j.cell.2015.06.001.

STAR★METHODS

KEY RESOURCES TABLE

REAGENT or RESOURCE	SOURCE	IDENTIFIER
Antibodies		
Rabbit polyclonal Muc2 antibody	Santa Cruz Biotechnology	Cat #: sc-15334; RRID: AB_2146667
Rabbit polyclonal Muc2 antibody	GeneTex	Cat #: GTX100664; RRID: AB_1950958
Goat polyclonal Muc2 antibody	Santa Cruz Biotechnology	Cat #: sc-13312; RRID: AB_2146672
Rabbit polyclonal Neu3 antibody	Santa Cruz Biotechnology	Cat #: sc-134931; RRID: AB_10609640
Rabbit polyclonal cathepsin G antibody, biotinylated	Biorbyt	Cat #: orb460740
Rabbit polyclonal cathepsin G antibody	Abcam	Cat #: ab197354
Rabbit monoclonal lysozyme antibody	Abcam	Cat #: ab108508; RRID: AB_10861277
Goat polyclonal αTubulin antibody	Santa Cruz Biotechnology	Cat #: sc-31779; RRID: AB_2210217
Rabbit polyclonal neutrophil elastase antibody	Cell Signaling Technology	Cat #: 44030
Rabbit polyclonal proteinase 3 antibody	LSBio	Cat #: LS-C296141
Erythrina cristagalli lectin, biotinylated	Vector Laboratories	Cat #: B-1145; RRID: AB_2336436
Ricinus Communis Agglutinin-I lectin, biotinylated	Vector Laboratories	Cat #: B-1085; RRID: AB_2336707
Peanut Agglutinin lectin, biotinylated	Vector Laboratories	Cat #: B-1075; RRID: AB_2313597
Maackia amurensis-II lectin, biotinylated	Vector Laboratories	Cat #: B-1265; RRID: AB_2336569
Sambucus nigra lectin, biotinylated	Vector Laboratories	Cat #: B-1305; RRID: AB_2336718
HRP-conjugated *Erythrina cristagalli* lectin	EY Laboratories	Cat #: H-5901-1
HRP-conjugated *Ricinus Communis Agglutinin*-I lectin	EY Laboratories	Cat #: H-2001-1
HRP-conjugated Peanut Agglutinin lectin	EY Laboratories	Cat #: H-2301-1
HRP-conjugated *Maackia amurensis*-II lectin	EY Laboratories	Cat #: H-7801-1
HRP-conjugated *Sambucus nigra* lectin	EY Laboratories	Cat #: H-6802-1
Texas Red-conjugated goat anti-rabbit IgG	Santa Cruz Biotechnology	Cat #: sc-2780; RRID: AB_ 649006
FITC-conjugated goat anti-rabbit IgG	Santa Cruz Biotechnology	Cat #: sc-2090; RRID: AB_ 641179
Texas Red-conjugated rabbit anti-goat IgG	Santa Cruz Biotechnology	Cat #: sc-3919; RRID: AB_ 654579
FITC-conjugated streptavidin	Vector Laboratories	Cat #: SA-5001; RRID: AB_ 2336462
HRP-conjugated streptavidin	BD Biosciences	Cat #: 550946
Bacterial and virus strains		
Salmonella enterica serovar Typhimurium	CDC 6516-60	ATCC 14028
Chemicals, peptides, and recombinant proteins		
10% buffered formalin	Sigma-Aldrich	Cat #: HT5014
Methanol	Sigma-Aldrich	Cat #: 179337
Chloroform	Sigma-Aldrich	Cat #: 34854
Acetic acid	Sigma-Aldrich	Cat #: 695092
Sucrose	Sigma-Aldrich	Cat #: S0389
Tissue-Tek OCT compound, Sakura Finetek	VWR	Cat #: 25608-930
Mayer's hematoxylin solution	Sigma-Aldrich	Cat #: MHS16
Eosin Y solution	Sigma-Aldrich	Cat #: HT110116
TRIzol Reagent	Invitrogen	Cat #: 15596026
Dextran-FITC	Sigma-Aldrich	Cat #: 68059
BD Microtainer Serum Separator Tube	BD Biosciences	Cat #: 365967
Protein A/G PLUS agarose	Santa Cruz Biotechnology	Cat #: sc-2003

(*Continued on next page*)

Continued

REAGENT or RESOURCE	SOURCE	IDENTIFIER
Amersham ECL Western Blotting Detection Reagent	GE Healthcare	Cat #: RPN2109
Coomassie brilliant blue G250	Bio-Rad	Cat #: 1610406
Precision Plus Protein™ Dual Color Standards	Bio-Rad	Cat #: 1610394
Bovine Serum Albumin (BSA)	Jackson ImmunoResearch	Cat #: 001-000-162
Sulfo-NHS-LC-LC-Biotin	ThermoFIsher Scientific	Cat #: 21335
3,3′,5,5′-Tetramethylbenzidine (TMB) Liquid Substrate	Sigma-Aldrich	Cat #: T0440
Zanamivir	Sigma-Aldrich	Cat #: SML0492
Complete protease inhibitor cocktail	Roche	Cat #: 11697498001
E−64	Sigma-Aldrich	Cat #: E3132
PMSF	Sigma-Aldrich	Cat #: P7626
EDTA	Sigma-Aldrich	Cat #: E9884
EGTA	Sigma-Aldrich	Cat #: E3889
Cathepsin G inhibitor	Sigma-Aldrich	Cat #: 219372
Elastase inhibitor	Sigma-Aldrich	Cat #: M0398
Trypsin inhibitor	Sigma-Aldrich	Cat #: T7254
Neuraminidase (from *Arthrobacter ureafaciens*)	EY Laboratories	Cat #: EC-32118-5
Critical commercial assays		
Hemoccult Fecal Blood Slide Test System	Beckman Coulter	Cat #: 60151
Alcian Blue Stain Kit	Vector Laboratories	Cat #: H-3501
Ulysis Alexa Fluor 488 Nucleic Acid Labeling Kit	Molecular Probes	Cat #: U21650
SuperScript III reverse transcriptase kit	Invitrogen	Cat #: 18080093
Brilliant SYBR green qPCR master mix kit	Agilent Technologies	Cat #: 600830
Amplex Red Neuraminidase Assay Kit	Thermo Fisher Scientific	Cat #: A22178
QIAamp DNA Mini Kit	Qiagen	Cat #: 51304
Experimental models: Organisms/strains		
C57BL/6J mice	The Jackson Laboratory	N/A
Neu3$^{-/-}$ mice	Yamaguchi et al.[30]	N/A
St3gal6$^{\Delta/\Delta}$ mice	Yang et al.[31]	N/A
Ctsg $^{-/-}$ mice	MacIvor et al.[15]	N/A
Tlr4$^{-/-}$ mice (B6(Cg)-Tlr4$^{tm1.2Karp}$/J)	The Jackson Laboratory	Stock #: 029015
Oligonucleotides		
EUB-338: GCTGCCTCCCGTAGGAGT	Gerlach et al.[33]	N/A
Non-EUB-338: CGACGGAGGGCATCCTCA	Gerlach et al.[33]	N/A
CCL5-forward: TCGTGTTTGTCACTCGAAGG	Yang et al.[9]	N/A
CCL5-reverse: CTAGCTCATCTCCAAATAGT	Yang et al.[9]	N/A
IL-1β-forward: GCCCATCCTCTGTGACTCAT	Yang et al.[9]	N/A
IL-1β-reverse: AGGCCACAGGTATTTTGTCG	Yang et al.[9]	N/A
TNFα-forward: CATCTTCTCAAAATTCGAGT	Yang et al.[9]	N/A
TNFα-reverse: TTTGAGATCCATGCCGTTGG	Yang et al.[9]	N/A
Muc2-forward: GCTGACGAGTGGTTGGTGAATG	Man et al.[37]	N/A
Muc2-reverse: GATGAGGTGGCAGACAGGAGAC	Man et al.[37]	N/A
CatG-forward: CAAGGAGATGAGGCAGGGAA	This paper	N/A
CatG-reverse: TGAGCTGCTGTTAGGACGAA	This paper	N/A
NE-forward: TGGCCTCAGAGATTGTTGGT	This paper	N/A
NE-reverse: TACCTGCACTGACCGGAAAT	This paper	N/A

(*Continued on next page*)

Continued

REAGENT or RESOURCE	SOURCE	IDENTIFIER
PR3-forward: AATGACGTGCTTCTCCTCCA	This paper	N/A
PR3-reverse: GTGACGTTCAGTTCCTGCAG	This paper	N/A
GAPDH -forward: TGGTGAAGGTCGGTGTGAAC	Yang et al.[12]	N/A
GAPDH -reverse: AGTGATGGCATGGACTGTGG	Yang et al.[12]	N/A
Total bacteria-forward: GTGCCAGCMGCCGCGGTAA	Fuhrer et al.[36]	N/A
Total bacteria-reverse: GACTACCAGGGTATCTAAT	Fuhrer et al.[36]	N/A
Clostridiaceae-forward: TTAACACAATAAGTWATCCACCTGG	Fuhrer et al.[36]	N/A
Clostridiaceae-reverse: ACCTTCCTCCGTTTTGTCAAC	Fuhrer et al.[36]	N/A
Lactobacillaceae-forward: AGCAGTAGGGAATCTTCC	Fuhrer et al.[36]	N/A
Lactobacillaceae-reverse: CGCCACTGGTGTTCYTCCATATA	Fuhrer et al.[36]	N/A
Bacteroidaceae-forward: CCAATGTGGGGGACCTTC	Fuhrer et al.[36]	N/A
Bacteroidaceae-reverse: AACGCTAGCTACAGGCTT	Fuhrer et al.[36]	N/A
Enterobacteriaceae-forward: CATTGACGTTACCCGCAGAAGAAGC	Fuhrer et al.[36]	N/A
Enterobacteriaceae-reverse: CTCTACGAGACTCAAGCTTGC	Fuhrer et al.[36]	N/A
Software and algorithms		
GraphPad Prism 7.0	GraphPad Software	https://www.graphpad.com/scientific-software/prism/
Microsoft Excel	Microsoft	https://products.office.com/en-us/excel
TissueFAXS imaging software 3.5	TissueGnostics imaging solution	http://www.tissuegnostics.com/en/products/imaging-software/170-tissuefaxs-imaging-software
TissueQuest Analysis software 4.0	TissueGnostics imaging solution	http://www.tissuegnostics.com/en/products/analysing-software/tissuequest
HistoQuest Analysis software 4.0	TissueGnostics imaging solution	http://www.tissuegnostics.com/en/products/analysing-software/histoquest
LabWorks Image Acquisition and Analysis Software	UVP	https://www.uvp.com/
ImageJ	NIH	https://ImageJ.nih.gov

RESOURCE AVAILABILITY

Lead contact

Further information and requests for resources and reagents should be directed to and will be fulfilled by the lead contact, Jamey D. Marth (jmarth@sbpdiscovery.org).

Materials availability

This study did not generate new unique reagents.

Data and code availability

- All data reported in this paper will be shared by the lead contact upon request.

- This paper does not report original code.
- Any additional information required to reanalyze the data reported in this paper is available from the lead contact upon request.

EXPERIMENTAL MODEL AND STUDY PARTICIPANT DETAILS

Laboratory animals

Animal experiments were used equal numbers of male and female mice, unless otherwise indicated. Inbred C57BL/6J mice were used (Jackson Laboratory). *Neu3*-deficient, *St3gal6*-deficient, and *Ctsg*-deficient mice were backcrossed six or more generations into the C57BL/6J background prior to study.[15,30,31] *Tlr4*$^{-/-}$ mice (B6(Cg)-Tlr4$^{tm1.2Karp}$/J) were purchased from the Jackson Laboratory. Littermates of the indicated genotypes were used as controls. Adult mice 8 weeks of age or older as indicated were used in all studies. Mice of both sexes were also used in approximately equal fractions. We found that the phenotypes and results obtained in our studies were not significantly different among adult males and females. All mice analyzed were provided sterile pellet food and water *ad libitum*. Institutional Animal Care and Use Committees of the University of California Santa Barbara and the Sanford-Burnham-Prebys Medical Discovery Institute approved the mouse studies undertaken herein. All mice were housed with their littermates typically in groups of four or five animals per cage in a specific pathogen-free barrier facility at the University of California Santa Barbara and the Sanford-Burnham-Prebys Medical Discovery Institute. Every effort was made to minimize and eliminate animal suffering and to reduce the number of animals needed.

Bacterial strains and culture conditions

MT2057, a kanamycin-resistant derivative of *Salmonella* enterica serovar Typhimurium (*ST*) reference strain ATCC 14028 (CDC 6516-60) was used.[9,32] *ST* was streaked from frozen stocks onto Luria-Bertani (LB) agar plates and incubated overnight at 37°C. Single colonies were inoculated into LB broth and incubated overnight with shaking at 37°C. *ST* was pelleted by centrifugation, washed, and suspended in sterile 0.2M sodium phosphate buffer (pH 8.1).

METHOD DETAILS

Bacterial infections

For the induction of chronic colitis, Adult 8-week-old mice were infected with *ST* (2×10^3 cfu) via gastric intubation at 4-week intervals successively up to five times during adult life after the initial infection.[9] Mice were weighed bi-weekly and further assessed for overt signs including the presence of diarrhea and fecal blood (Hemoccult Fecal Blood Slide Test System, Beckman Coulter).[9,21]

Histology

Mouse intestinal tissues were fixed in 10% buffered formalin (Sigma-Aldrich) or Methanol-Carnoy's fixative, transferred to 30% sucrose/PBS, and embedded in Tissue-Tek OCT compound (Sakura Finetek).[5,21,33] Three-micron frozen sections were stained with hematoxylin and eosin (H&E; Sigma-Aldrich) or incubated with 1 μg/ml of antibodies to one or more molecules including Muc2 (H-300, Santa Cruz Biotechnology), Neu3 (M-50, Santa Cruz Biotechnology), cathepsin G (orb460740, Biorbyt), lysozyme (EPR2994(2), Abcam), or αTubulin (P-16, Santa Cruz Biotechnology), or 5 μg/ml of biotinylated lectins including *Erythrina cristagalli* (ECA), *Ricinus Communis* Agglutinin-I (RCA), Peanut Agglutinin (PNA), *Maackia amurensis*-II (MAL-II), or *Sambucus nigra* (SNA) (Vector Laboratories). Tissue sections were also stained with Alcian blue, followed by counterstaining with nuclear fast red (Vector Laboratories). Muc2 or lysozyme was visualized with 0.4 μg/ml of Texas Red-conjugated goat anti-rabbit IgG secondary antibodies (Santa Cruz Biotechnology); Neu3 was visualized with 0.4 μg/ml of FITC-conjugated goat anti-rabbit IgG secondary antibodies (Santa Cruz Biotechnology); αTubulin was visualized with 0.4 μg/ml of Texas Red-conjugated rabbit anti-goat IgG secondary antibodies (Santa Cruz Biotechnology); and cathepsin G or biotinylated lectins were visualized with 1 μg/ml of FITC-conjugated streptavidin (Vector Laboratories). These primary antibody or lectin incubations were performed at 4°C overnight and secondary antibody or streptavidin incubations were performed at room temperature for 1 h. For fluorescence *in situ* hybridization (FISH), colon sections fixed with Methanol-Carnoy's fixative were incubated with of 250 μg of Alexa Fluor 488–conjugated EUB-338 (5′-GCTGCCTCCCGTAGGAGT-3′; bp 337–354 in bacteria EU622773) or a control nonspecific probe complementary to EUB-338 (Non-EUB-338; 5′-CGACGGAGGGCATCCTCA-3′) in 100 μl hybridization buffer (20 mM Tris-HCl (pH 7.4), 0.9 M NaCl, and 0.1% SDS) at 50°C overnight.[33] The sections were rinsed in wash buffer (20 mM Tris-HCl (pH 7.4) and 0.9 M NaCl) at 50°C for 15 min and co-immunostained with 1 μg/ml of antibody to Muc2 (H-300, Santa Cruz Biotechnology) at 4°C. Analyses by microscopy was performed using a TissueGnostics workstation equipped with Zeiss AxioImager Z1, Hamamatsu C13440-20C camera, PixeLINK PL-D673CU camera, and Lumen Dynamics X-Cite XLED1 illuminator. Images collected were analyzed using TissueFAXS (Version 3.5), TissueQuest (Version 4.0), HistoQuest software (Version 4.0) (TissueGnostics USA Ltd.), and ImageJ software (Version 2.0.0) (NIH).

mRNA preparation and quantification by real-time PCR

Total RNA was isolated from tissues using Trizol (Invitrogen) and subjected to reverse transcription (RT) using SuperScript III (Invitrogen). Quantitative real-time PCR was performed using Brilliant SYBR Green Reagents with the Mx3000P QPCR System (Stratagene). Primers used for real-time PCR in the mouse were: CCL5-RT-F (5′-TCGTGTTTGTCACTCGAAGG-3′), CCL5-RT-R (5′-CTAGCTCATCTCCAAATAGT-3′), IL-1β-RT-F (5′-GCCCATCCTCTGTGACTCAT-3′), IL-1β-RT-R (5′-AGGCCACAGGTATTTTGTCG-3′), TNFα-RT-F (5′-CATCTTCTCAAAAT

TCGAGT-3′), TNFα-RT-R (5′-TTTGAGATCCATGCCGTTGG-3′), Muc2-RT-F (5′-GCTGACGAGTGGTTGGTGAATG-3′), Muc2-RT-R (5′-GATGAGGTGGCAGACAGGAGAC-3′), CatG-RT-F (5′-CAAGGAGATGAGGCAGGGAA-3′), CatG-RT-R (5′-TGAGCTGCTGTTAGGACGAA-3′), NE-RT-F (5′-TGGCCTCAGAGATTGTTGGT-3′), NE-RT-R (5′-TACCTGCACTGACCGGAAAT-3′), PR3-RT-F (5′-AATGACGTGCTTCTCCTCCA-3′), PR3-RT-R (5′-GTGACGTTCAGTTCCTGCAG-3′), GAPDH-RT-F (5′-TGGTGAAGGTCGGTGTGAAC-3′), and GAPDH-RT-R (5′-AGTGATGGCATGGACTGTGG-3′). Relative mRNA levels were normalized to expression of *Gapdh* RNA.

In vivo intestinal barrier function

Dextran-FITC (Sigma-Aldrich) was administered via oral gavage (600 mg/kg), blood was collected from anesthetized animals into Microtainer Serum Separator Tubes (BD Biosciences) at 4 h with no anticoagulant, and allowed to clot for 30 min at room temperature.[34] Serum was collected after centrifugation at 10,000 × *g* for 10 min. The amount of FITC in each sample was measured by using a Spectra Max Gemini EM fluorescent plate reader (Molecular Devices) at 490 and 530 nm for the excitation and emission wavelengths, respectively.

Separation of loose and stratified mucus layer Muc2

Mucus from the colon was removed from an identically measured epithelial surface by suction (loosely adherent) or scraped (firmly adherent).[5] The samples were homogenized in radioimmunoprecipitation assay (RIPA) buffer (50 mM Tris-HCl (pH 7.6), 150 mM NaCl, 1 mM EDTA, 1% NP-40, 1% sodium deoxycholate, and 0.1% SDS) supplemented with complete protease inhibitor cocktail per instructions (Roche). Muc2 proteins in loose and stratified mucus layer were analyzed by immunoblotting using 1 μg/ml of antibody to Muc2 (C3, GeneTex) or immunoprecipitated with 2 μg/ml of antibody to Muc2 (R-12, Santa Cruz Biotechnology).

Immunoprecipitation, immunoblotting, and lectin blotting

Tissue samples were homogenized in RIPA buffer supplemented with complete protease inhibitor cocktail per instructions (Roche) and incubated overnight at 4°C on a rotating wheel with 2 μg/ml of antibody to Muc2 (R-12, Santa Cruz Biotechnology), followed by 2 h of incubation in the presence of protein A/G PLUS agarose (Santa Cruz Biotechnology). Immunoprecipitates were washed five times with RIPA buffer and eluted with SDS sample buffer. Protein samples eluted or total tissue homogenates were subjected to SDS-PAGE, transferred to nitrocellulose membranes, and incubated with 3% BSA in Tris-buffered saline (TBS). They were then analyzed by immunoblotting using 1 μg/ml of antibody to Muc2 (C3, GeneTex), cathepsin G (ab197354, Abcam), neutrophil elastase (44030, Cell Signaling Technology), or proteinase 3 (LS-C296141, LSBio) or by lectin blotting with HRP-conjugated ECA (0.5 μg/ml), RCA (0.1 μg/ml), PNA (1 μg/ml), MAL-II (0.2 μg/ml), or SNA (0.1 μg/ml) (EY Laboratories). Signals detected by chemiluminescence (GE Healthcare) were analyzed by integrated optical density using LabWorks Image Acquisition and Analysis Software (UVP Bioimaging Systems). Parallel protein samples were visualized with Coomassie brilliant blue G250 staining (Bio-Rad). Protein standards prestained, broad range 250–10 kDa were used as molecular weight markers (1610394, Bio-rad).

ELISA

ELISA plates (Nunc) were coated with 2 μg/ml of antibodies to Muc2 (R-12, Santa Cruz Biotechnology) and blocked by incubation at room temperature for 1 h with 5% BSA in PBS (Jackson ImmunoResearch). To generate biotinylated antigens, 500 μl of total protein extracts isolated from mouse tissue (1 mg/ml) were incubated with 500 μl of sulfo-NHS-LC-LC-biotin (1 mg/ml) (Thermo Fisher Scientific) on ice for 2 h and the biotinylation reaction was stopped with the addition of 15 mM glycine (pH 8.0; final concentration). After washing the ELISA plates, 20 μg of biotinylated protein extracts was added to each well and incubated at room temperature for 2 h. Antigens were detected following the addition of 1:5000 dilution of HRP-streptavidin (BD Biosciences) and 3,3′,5,5′ tetramethylbenzidine (TMB, Sigma-Aldrich). Lectin binding was determined in parallel by the addition of HRP-conjugated ECA (0.5 μg/ml), RCA (0.1 μg/ml), PNA (1 μg/ml), MAL-II (0.2 μg/ml), or SNA (0.1 μg/ml) (EY Laboratories), followed by TMB, and changes in glycan linkages were detected by comparing lectin binding among identical amounts of biotinylated Muc2.[35]

Neuraminidase activity and inhibition

Neuraminidase activity was measured in tissue extracts in RIPA buffer supplemented with complete protease inhibitor cocktail per instructions (Roche) using the Amplex Red Neuraminidase Assay Kit according to the manufacturers' instructions (Molecular Probes). For inhibition of neuraminidase activity in the colon, Zanamivir (0.5 mg/ml; Sigma-Aldrich) was provided in the drinking water immediately following the initial *ST* infection at 8 weeks of age and continued for the duration of study as indicated.

In vitro Muc2 proteolysis

For obtaining Muc2 immunoprecipitates, 1 mg of tissue lysates in RIPA buffer from the colonic stratified layer of indicated genotypes at 12 weeks of age was incubated overnight at 4°C with 2 μg/ml of antibody to Muc2 (R-12, Santa Cruz Biotechnology), followed by 2 h of incubation in the presence of protein A/G PLUS agarose and washed five times with RIPA buffer. For producing the Muc2-depleted intestinal content solution, 100 mg of intestinal content from wild-type mice at 20 weeks of age following *ST* re-infection or PBS administration was diluted in 1 ml of TBS buffer and vortexed thoroughly to make an intestinal content solution. After centrifugation at 14,000 rpm, the supernatants was incubated with 2 μg/ml of Muc2 antibody (R-12, Santa Cruz Biotechnology) and protein A/G PLUS agarose for 2 h at room

temperature, centrifuged at 2,000 rpm to remove agarose beads, and then applied to Poly-Prep gravity-flow columns (Bio-rad). The flow-through fractions were incubated with Muc2 antibody and protein A/G PLUS agarose, centrifuged at 2,000 rpm to remove agarose beads, and then applied to Poly-Prep gravity-flow columns and these steps were repeatedly performed until Muc2 proteins were not detected in the final flow-through fractions. For *in vitro* Muc2 proteolysis assay, Muc2 immunoprecipitates isolated from the colonic stratified layer of indicated genotypes at 12 weeks of age were mixed with 1 ml of Muc2-depleted lumenal extract solution generated from 100 mg of lumenal content of WT mice at 20 weeks of age prior to the fourth *ST* infection or PBS treatment. After incubation in a shaking incubator at 37°C for the indicated times otherwise 24 h, Muc2 immunoprecipitates were washed five times with RIPA buffer, eluted with SDS sample buffer, and subjected to immunoblotting. For protease activity inhibition, complete protease inhibitor cocktail per instructions (Roche), 1 mM E-64 (Sigma-Aldrich), 1 mM PMSF (Sigma-Aldrich), 1 mM EDTA/EGTA (Sigma-Aldrich), 100 μM cathepsin G inhibitor (CAS 429676-93-7; Sigma-Aldrich), 100 μM neutrophil elastase inhibitor (CAS 65144-34-5; Sigma-Aldrich), or 100 μM trypsin inhibitor (CAS 4272-74-6; Sigma-Aldrich) was added to the *in vitro* Muc2 proteolysis assay.[23] For *in vitro* sialidase treatment, Muc2 immunoprecipitates were incubated with 0.3 U/ml of *Arthrobacter urefaciens* sialidase (EY lab) or PBS at 37°C for 2 h in the absence or presence of a sialidase inhibitor zanamivir (0.5 mg/ml; Sigma-Aldrich) and washed with TBS buffer prior to or after *in vitro* Muc2 proteolysis assay.

Comparative studies of intestinal microbiota

Total DNA was extracted from 1 mg of intestinal content or colon tissue per individual mouse using QIAamp DNA Mini Kit according to the manufacturer's instructions (Qiagen). Total DNA was quantified and used as the template for quantitative real-time PCR (qPCR). A subset of commensal microbial populations were analyzed with Brilliant SYBR Green Reagents and the Mx3000P QPCR System (Stratagene). Oligonucleotide primers for total bacterial DNA were (Total-F-5′-GTGCCAGCMGCCGCGGTAA-3′, Total-R-5′-GACTACCAGGGTATCTAAT-3′; while those to measure individual populations included *Clostridiaceae*-F-5′-TTAACACAATAAGTWATCCACCTGG-3′, *Clostridiaceae* -R-5′-ACCTTCCTCCGTTTTGTCAAC-3′; *Lactobacillaceae*-F-5′-AGCAGTAGGGAATCTTCC-3′, *Lactobacillaceae*-R-5′-CGCCACTGGTGTTCYTC CATATA-3′; *Bacteroidaceae*-F-5′-CCAATGTGGGGGACCTTC-3′, *Bacteroidaceae*-R-5′-AACGCTAGCTACAGGCTT-3′; and *Enterobacteriaceae*-F-5′-CATTGACGTTACCCGCAGAAGAAGC-3′, *Enterobacteriaceae*-R-5′-CTCTACGAGACTCAAGCTTGC-3′).[36] Serial dilutions of total DNA were used to generate standard curves in acquiring each measurement. Relative levels of bacterial DNA obtained per mg of intestinal content from each mouse were calculated in plotting comparisons to wild-type littermates.

QUANTIFICATION AND STATISTICAL ANALYSIS

All data were analyzed as mean ± SD. unless otherwise indicated. Student's unpaired *t* test was used to compare the means of two groups. One-way Analysis of Variance (ANOVA) with Tukey's multiple comparisons test was used to compute statistical significance between multiple groups. GraphPad Prism software (Version 7.0) was used to determine statistical significance among multiple studies. *P* values of less than 0.05 were considered significant. Statistical significance was denoted by $*P < 0.05$, $**P < 0.01$, or $***P < 0.001$. The exact value of n, representing the number of mice in the experiments depicted, was indicated in the figure legends.